Fizika Nizkikh Temperatur, 2008, v. 34, No. 7, p. 695–700

Nonlinear localized modes in complex chains and carbon nanotubes

A. Savin

Semenov Institute of Chemical Physics, Russian Academy of Sciences, Moscow 117977, Russia

Yu.S. Kivshar

Nonlinear Physics Center, Research School of Physical Sciences and Engineering
Australian National University, Canberra, ACT 0200, Australia
E-mail: ysk@internode.on.net

Received December 26, 2007

We discuss the existence of spatially localized nonlinear modes in carbon nanotubes with different chiralities, and demonstrate that in nanotubes with the chirality index $(m,0)$ three types of localized modes can exist, namely longitudinal, radial, and twisting nonlinear localized modes. We demonstrate that only the nonlinear modes associated with the twisting oscillations are nonradiating modes, and they exist in the frequency gaps of the linear spectrum. Geometry of carbon nanotubes with the index (m, m) allows only the existence of broad radial breathers in a narrow spectral range.

PACS: **61.48.–c** Structure of fullerenes and related hollow molecular clusters;
71.20.Tx Fullerenes and related materials; intercalation compounds;
71.45.Lr Charge-density-wave systems.

Keywords: carbon nanotubes, nonlinear modes, oscilations.

1. Introduction

Spatially localized modes in perfect nonlinear chains have been first discussed by A.M. Kosevich and A.S. Kovalev [1]; in the framework of the asymptotic method they found spatially localized in space and periodic in time solutions of the nonlinear equations describing oscillations of a linear chain of particles placed in an external potential. The similar physical objects have been introduced much later by A.J. Sievers and S. Takeno in the form of the so-called «intrinsic localized modes» [2], as solutions of the dynamic equations for nonlinearly coupled particles in a chain. Both types of spatially localized periodic modes appear in strongly nonlinear systems, and their spatial size may become comparable with the lattice spacing. Such nonlinear localized modes are also called *discrete breathers or discrete solitons* in other fields, and they are responsible for energy localization in the dynamics of discrete nonlinear lattices [3,4]. The manipulation of the discrete breathers has been achieved in systems as diverse as annular arrays of coupled Josephson junctions [5], optical waveguide arrays [6], and antiferromagnetic spin lattices [7]. The theoretical study and direct experimental observation of highly localized, stable, nonlinear excitations at the atomic level in complex nonlinear chains such as carbon nanotubes will underscore their importance in physical phenomena at all scales.

In this paper, we extend substantially the concept introduced long time ago by A.M. Kosevich and A.S. Kovalev, and study the energy localization in complex nonlinear discrete systems. In particular, we demonstrate that the standard model of carbon nanotubes with the index $(m,0)$ may support at least *three types* of different nonlinear localized modes, whereas nanotubes with the index (m,m) support only one type of discrete breather.

Carbon nanotubes [8] have attracted a considerable attention in recent years after their discovery by Iijima [9]. They can be thought of as complex multi-atom structures in the form of a cylinder of carbon atoms arranged in hexagonal grids similar to other types of fullerene-related structures. The growing interest to the study of carbon nanotubes can be explained by their unique physical properties and their potential for a wide range of possible applications. In particular, the carbon nanotubes are known for their superior mechanical strength [10] and

good heat conductance [11]. In addition, it is well established that C_{60} fullerenes can support large-amplitude oscillations [12] which can be excited and controlled by temporally shaped laser pulses [13].

In the continuum approximation, nonlinear dynamics of carbon nanotubes has been analyzed by several groups and, in particular, supersonic longitudinal compression solitons described by the effective Korteweg-de Vries equation have been predicted to exist in such structures, similar to other simpler discrete lattices [14]. However, the recent numerical modeling of more complete discrete model of carbon nanotubes has demonstrated [15] that acoustic solitons *do not exist* in such curved structures, and their supersonic motion is always accompanied by strong radiation of phonons.

Here we focus on the study of *large-amplitude* oscillating modes of carbon nanotubes that have the additional features of being *nonlinear* as well as *discrete*. We reveal that both nonlinearity and discreteness induce localization of anharmonic oscillations and, as a result, the combination of both leads to the generation of specific spatially localized modes of the type of discrete breathers [2,16]. These modes act like stable effective impurity modes that are dynamically generated and may alter dramatically many properties of carbon nanotubes.

The paper is organized as follows. First, in Sec. 2 we introduce our model and discuss its several simplifying reductions. Then, we find different types of localized modes in a planar structure of unfolded nanotubes (Sec. 3). Sec. 4 discusses the discrete modes in curved geometry, Sec. 5 we considered thermalized dynamics and Sec. 6 concludes the paper.

2. Effective model

The structure of a carbon nanotube is shown schematically in Fig. 1. In static, the nanotube is characterized by its radius R and two step parameters h_1 and h_2. In each layer, the nanotube has m atoms separated by the angular distance $\Delta\phi = 2\pi/m$, so that h_1 and h_2 define alternating longitudinal distances between the transverse layers. We consider such dynamics of the nanotube that all atoms in one transverse layer have identical displacements. In this case, the carbon nanotube can be modeled by an effective one-dimensional diatomic chain, where the coordinates of atoms $(\rho_{n,l}\cos\varphi_{n,l}, \rho_{n,l}\sin\varphi_{n,l}, z_n)$ are defined by the equations

$$\rho_{n,l} = R + r_n(t);\ \varphi_{n,l} = \Delta\phi(l-1) + \phi_n(t),$$
$$z_{n,l} = (2k-2)(h_1+h_2) + u_n(t) \ \text{ for } \ n = 4k-1;$$
$$\varphi_{n,l} = \Delta\phi(l-1) + \Delta\phi/2 + \phi_n(t),$$
$$z_{n,l} = (2k-2)(h_1+h_2) + h_1 + u_n(t) \ \text{ for } \ n = 4k;$$
$$\varphi_{n,l} = \Delta\phi(l-1) + \Delta\phi/2 + \phi_n(t),$$
$$z_{n,l} = (2k-1)(h_1+h_2) + u_n(t) \ \text{ for } \ n = 4k+1; \text{ and}$$
$$\varphi_{n,l} = \Delta\phi(l-1) + \phi_n(t),$$
$$z_{n,l} = (2k-1)(h_1+h_2) + h_1 + u_n(t) \text{ for } n = 4k+2,$$

where the index $n = 4k+i$, $(k = 0, \pm1, \pm2, \ldots,\ i = -1, 0, 1, 2)$ stands for the number of the transverse atomic layer, the index $l = 1, \ldots, m$ marks an atom in the transverse layer, $r_n(t)$ is a relative change of the radius of the n-th transverse layer, ϕ_n is the angle of rotation of the atoms in the layer, and u_n is a relative longitudinal displacement of the atoms from their equilibrium position. In the static case, $r_n \equiv 0$, $\phi_n \equiv 0$, and $u_n \equiv 0$.

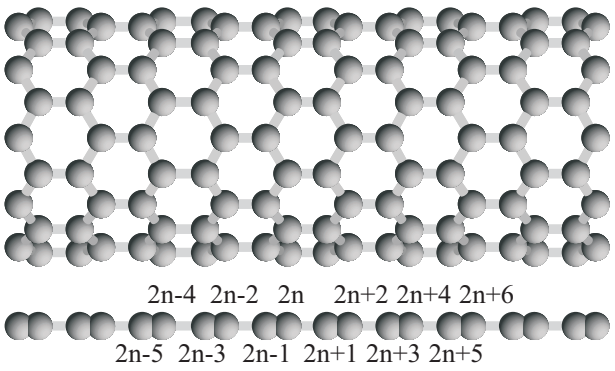

Fig. 1. Schematic of a carbon nanotube with the index (m,0). Below: an effective one-dimensional diatomic chain.

In this case, complex three-dimensional dynamics of a nanotube can be reduced to the analysis of an effective one-dimensional three-component chain model with two atoms per its unit cell, and Hamiltonian of this model can be written in the form,

$$H = \sum_n [E_{2n} + E_{2n+1} + Z(\mathbf{y}_{2n-2}; \mathbf{y}_{2n-1}; \mathbf{y}_{2n}; \mathbf{y}_{2n+1})], \tag{1}$$

where $E_n = M[\dot r_n^2 + (R+r_n)^2\dot\phi_n^2 + \dot u_n^2]/2$ is the kinetic energy , M is the mass of a carbon atom (the total energy of the nanotube is mH), and the vector $\mathbf{y}_n = (r_n, \phi_n, u_n)$. The interatomic potential can be written in the form,

$$Z(\mathbf{y}_1, \mathbf{y}_2, \mathbf{y}_3, \mathbf{y}_4) = V(\mathbf{x}_1, \mathbf{x}_2) + V(\mathbf{x}_2, \mathbf{x}_3) + V(\mathbf{x}_2, \mathbf{x}_4) +$$
$$+ U(\mathbf{x}_2, \mathbf{x}_3, \mathbf{x}_5) + U(\mathbf{x}_6, \mathbf{x}_3, \mathbf{x}_2) + U(\mathbf{x}_6, \mathbf{x}_3, \mathbf{x}_5) +$$
$$+ U(\mathbf{x}_1, \mathbf{x}_2, \mathbf{x}_3) + U(\mathbf{x}_1, \mathbf{x}_2, \mathbf{x}_4) + U(\mathbf{x}_3, \mathbf{x}_2, \mathbf{x}_4) +$$
$$+ W(\mathbf{x}_6, \mathbf{x}_3, \mathbf{x}_2, \mathbf{x}_5) + W(\mathbf{x}_6, \mathbf{x}_3, \mathbf{x}_5, \mathbf{x}_2) + W(\mathbf{x}_2, \mathbf{x}_3, \mathbf{x}_6, \mathbf{x}_5) +$$
$$+ W(\mathbf{x}_1, \mathbf{x}_2, \mathbf{x}_4, \mathbf{x}_3) + W(\mathbf{x}_1, \mathbf{x}_2, \mathbf{x}_3, \mathbf{x}_4) + W(\mathbf{x}_3, \mathbf{x}_2, \mathbf{x}_1, \mathbf{x}_4),$$

where the coordinate vectors $\mathbf{x}_i = (x_i, y_i, z_i)$, $i = 1, 2, \ldots, 6$ are defined as:

$$x_6 = (R + r_1)\cos(\Delta\phi + \phi_1),\ y_6 = (R + r_1)\sin(\Delta\phi + \phi_1),$$
$$z_6 = -h_2 + u_1,\ x_1 = (R + r_2)\cos(\phi_2),$$
$$y_1 = (R + r_2)\sin(\phi_2),\ z_1 = u_2,\ x_3 = (R + r_2)\cos(\Delta\phi + \phi_2),$$
$$y_3 = (R + r_2)\sin(\Delta\phi + \phi_2),\ z_3 = u_2,$$
$$x_2 = (R + r_3)\cos(\Delta\phi/2 + \phi_3),$$
$$y_2 = (R + r_3)\sin(\Delta\phi/2 + \phi_3),\ z_2 = h_1 + u_3,$$
$$x_5 = (R + r_3)\cos(3\Delta\phi/2 + \phi_3),$$
$$y_5 = (R + r_3)\sin(3\Delta\phi/2 + \phi_3),\ z_5 = h_1 + u_3,$$
$$x_4 = (R + r_4)\cos(\Delta\phi/2 + \phi_4),$$
$$y_4 = (R + r_4)\sin(\Delta\phi/2 + \phi_4),\ z_4 = h_1 + h_2 + u_4.$$

The potential $V(\mathbf{x}_1, \mathbf{x}_2) = D\{\exp(-\alpha[\rho - \rho_0]) - 1\}^2$, $\rho = |\mathbf{x}_2 - \mathbf{x}_1|$, describes a change of the deformation energy due to interaction between two atoms with the coordinates $\mathbf{x}_1$ and $\mathbf{x}_2$. Potential $U(\mathbf{x}_1, \mathbf{x}_2, \mathbf{x}_3) = \varepsilon_v(\cos\varphi + 1/2)^2$, where $\cos\varphi = (\mathbf{v}_1, \mathbf{v}_2)/(|\mathbf{v}_1| \cdot |\mathbf{v}_2|)$, and $\mathbf{v}_1 = \mathbf{x}_2 - \mathbf{x}_1$, $\mathbf{v}_2 = \mathbf{x}_3 - \mathbf{x}_2$, describes the deformation energy of the angle between the links $\mathbf{x}_1\mathbf{x}_2$ and $\mathbf{x}_2\mathbf{x}_3$. Finally, the potential $W(\mathbf{x}_1, \mathbf{x}_2, \mathbf{x}_3, \mathbf{x}_4) = \epsilon_t(1 - \cos\phi)$, where $\cos\phi = (\mathbf{u}_1, \mathbf{u}_2)/(|\mathbf{u}_1| \cdot |\mathbf{u}_2|)$ and $\mathbf{u}_1 = (\mathbf{x}_2 - \mathbf{x}_1) \times (\mathbf{x}_3 - \mathbf{x}_2)$, $\mathbf{u}_2 = (\mathbf{x}_3 - \mathbf{x}_2) \times (\mathbf{x}_4 - \mathbf{x}_3)$, describes the deformation energy associated with a change of the effective angle between the planes $\mathbf{x}_1\mathbf{x}_2\mathbf{x}_3$ and $\mathbf{x}_2\mathbf{x}_3\mathbf{x}_4$. We take the mass of carbon atom as $M = 12\, m_p$, where m_p if the proton mass, the length $\rho_0 = 1.418$ Å, and energy $D = 4.9632$ eV. Other model parameters such as α, ε_v, and ε_t can be determined from the phonon frequency spectrum of a plane of carbon atoms.

3. Breathers in a planar system

A flat plane of the carbon atoms (graphene) is a special case of carbon nanotubes in the limit R, when $h_1 = \rho_0/2$ and $h_2 = \rho_0$. For such a plane the motion equation splits into the equations for longitudinal and transverse motion. The corresponding Hamiltonian takes a simpler form,

$$H = \sum_n \left[\frac{1}{2} M(\dot{u}_{2n-1}^2 + \dot{u}_{2n}^2) + V_1(\rho_{2n}) + V_2(\rho_{2n-1}) \right], \tag{2}$$

where $\rho_n = u_{n+1} - u_n$, the potentials

$$V_1(w) = D[\exp(-\alpha w) - 1]^2,$$
$$V_2(w) = 2D\{\exp(-\alpha[a_+(w)^{1/2} - \rho_0]) - 1\}^2 +$$
$$+ 2\varepsilon_v[a_-(w)/a_+(w) + 1/2]^2 +$$
$$+ 4\varepsilon_v[(w + \rho_0/2)/\sqrt{a_+(w)} - 1/2]^2,$$

and function $a_\pm(w) = (w + \rho_0/2)^2 \pm 3\rho_0^2/4$.

The stiffness parameters of the potentials are $K_1 = V_1''(0) = 2D\alpha^2$ and $K_2 = V_2''(0) = D\alpha^2 + 27\varepsilon_v/2\rho_0^2$. After linearizing the equation of motion following from the Hamiltonian (2), we obtain the dispersion relation for longitudinal phonons, $\omega_\pm(q) = \{(K_1 + K_2 \pm [(K_1 + K_2)^2 - 2K_1K_2(1 - \cos 2q)]^{1/2})/M\}^{1/2}$, which are depicted in Fig. 2. The frequency spectrum consists of the acoustic $[\omega_-(0), \omega_-(\pi/2)]$ and optical $[\omega_+(\pi/2), \omega_+(0)]$ bands where $\omega_-(0) = 0$, $\omega_+(0) = \sqrt{2(K_1 + K_2)/M}$, $\omega_-(\pi/2) = \sqrt{2K_2/M}$, and $\omega_+(\pi/2) = \sqrt{2K_1/M}$.

The edge frequencies of the optical band can be estimated from the experimental data: $\omega_+(\pi/2) \approx 1200$ cm^{-1} and $\omega_+(0) \approx 1600$ cm^{-1} [17]. These values allow us to determine the stiffness parameters, $K_1 = 508.98$ N/m and $K_2 = 395.87$ N/m, and find the maximum frequency of acoustic phonons, $\omega_-(\pi/2) = 1058.3$ cm^{-1}. Knowing the values of K_1 and K_2, we then find other parameters, $\alpha = 1.7889$ Å^{-1} and $\varepsilon_v = 1.3143$ eV. The value of the torsion potential ε_t can be evaluated from the maximum frequency of the transverse oscillations of a plane carbon lattice. For $\varepsilon_t = 0.2$ eV, we find the value 570 cm^{-1}. In order to find the parameters R, h_1, and h_2, we should solve the minimum problem $Z(\mathbf{0}, \mathbf{0}, \mathbf{0}, \mathbf{0}) \to \min\{R, h_1, h_2\}$. The resulting value of energy is then used as the minimum value.

A simple form of the Hamiltonian (1) allows to obtain analytical results for the nonlinear dynamics similar to the case of diatomic lattices. These results allow to predict the existence of discrete breathers with the frequencies below the lowest optical frequency of the longitudinal phonons (see Fig. 2,*c*)]. The form of this breather is

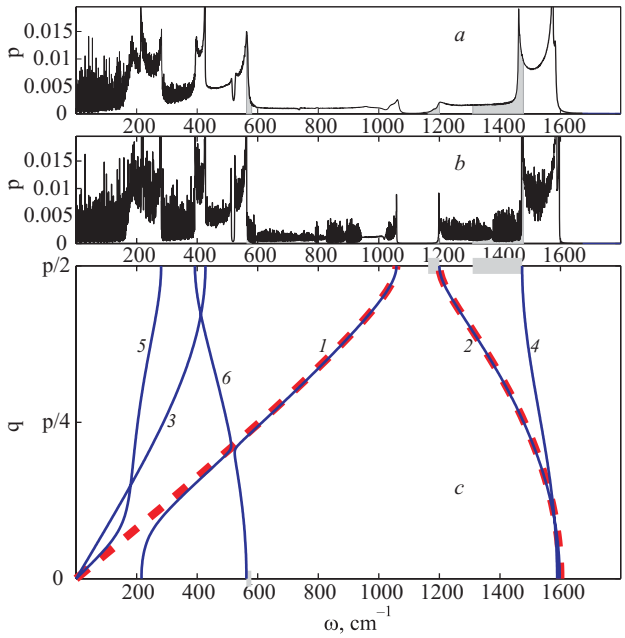

Fig. 2. Spectral density of thermal oscillations of a carbon nanotube (10,0) for the temperature T, K: 300 (*a*) and 30 (*b*). Dispersion curves of the phonons: acoustic (*1*) and optical (*2*) longitudinal phonons, acoustic (*3*) and optical (*4*) rotation phonons, and acoustic (*5*) and optical (*6*) radial phonons. For comparison, dashed lines show the dispersion curves of longitudinal oscillations of a plane of carbon. Light areas mark the frequency spectrum of breathers (*c*) .

shown in Fig. 3. The breather is characterized by the frequency ω, energy E, width of the localization region, L, and the chain extension A. The breather frequency is inside the band (1162, 1200) cm^{-1} near the lowest edge of the longitudinal optical oscillations. For decreasing ω, both E and A grow monotonically, and the breather width decreases.

Hamiltonian (1) defines the motion equations of the system. We have studied these equations numerically and revealed that they support the existence of *three types* of strongly localized nonlinear modes — *discrete breathers*. The first type, *longitudinal breathers*, also exists in planar carbon structures, such breathers exist in the frequency range [1162, 1200] cm^{-1}. The second type, *radial breathers*, describes transverse localized nonlinear modes with the frequency band [562, 580] cm^{-1}. The third type, *twisting breathers*, characterizes localization of the torsion oscillations of the nanotube with the frequencies [1310, 1477] cm^{-1}. The frequency spectra of the breathers are shown in Fig.2.

4. Breathers in the curved geometry

For a flat plane of carbon atoms, the longitudinal breathers are nonlinear modes (see Figs. 3,*a*,*c*), and they are exact solutions of the nonlinear motion equations. However, in the case of a curved geometry, the longitudinal breathers become coupled to transverse linear modes, and they always emit some radiation. This radiation is defined by the curvature of the nanotube and its index m. Therefore, the longitudinal breathers are not genuine nonlinear modes of carbon nanotubes, and they possess a finite lifetime which however may exceed a few hundred of picoseconds.

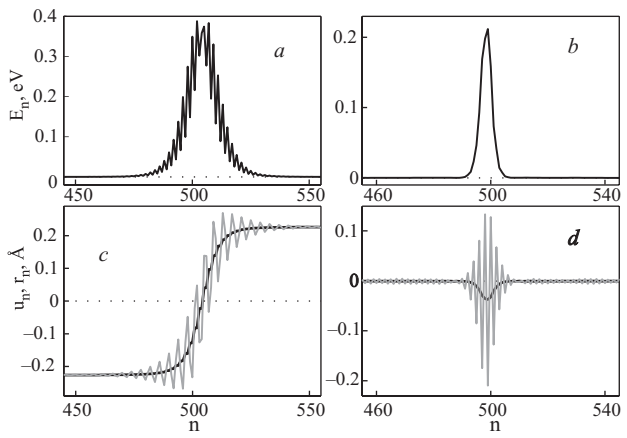

Fig. 3. Example of a localized nonlinear mode of the longitudinal oscillations described by the Hamiltonian (2) (*a*), (*b*) (frequency $\omega = 1164$ cm^{-1}, energy $E = 5.71$ eV, width $L = 16.3$, the chain extension $A = 0.45$ Å) and example of a radial breather (*c*), (*d*) describing localized transverse oscillations of a nanotube (10,0) with the frequency $\omega = 579.6$ cm^{-1}, energy $E = 0.99853$ eV, and width $L = 32.7$. Shown are (*a*) and (*c*) the averaged (in time) energy distribution E_n in the chain, (*b*) the atom displacements u_n, and (*d*) transverse displacements r_n. In Sec. (*b*) and (*d*) black lines show the values averaged over the period, light lines — maximal displacements. Radiation of longitudinal waves by a radial breather is clearly visible in Sec. (*d*).

The second type of discrete breathers we found is associated with the localization of transverse radial oscillations of a nanotube. Example of this radial breather in the nanotube (10,0) is shown in Figs. 3,*b*,*d*. Localized out-phase transverse oscillations of the neighboring atoms lead to localized contraction and extension of the nanotube. Such transverse oscillations become coupled to the longitudinal oscillations and, therefore, the radial breathers radiate longitudinal phonons. As a result, the radial breathers are also not genuine nonlinear localized modes of the carbon nanotubes, and they decay slow by emitting small-amplitude phonons. The lifetime of these breathers can be of the order of several nanoseconds.

The third type of localized mode is a twisting breather, or *twiston*, associated with the torsion oscillations of the nanotube. In a sharp contrast to other two breathing modes, the twisting breather is an exact solution of the motion equations of the nanotube, and it does not radiate phonons. An example of this genuine discrete breather is shown in Fig. 4. In the localized region of this mode, the nanotube is expanded transversally being contracted longitudinally. The twiston has a broad frequency spectrum, and its energy, amplitude of the transverse extension (see Fig. 5), and the amplitude of torsion oscillations all grow with the frequency. The breather width changes monotonically, and for the frequencies $\omega < 1450$ cm^{-1} it becomes comparable with the lattice spacing, so that the breather becomes a highly localized mode.

5. Thermalized dynamics

Next, we analyze thermal oscillations of a carbon nanotube by employing the Langevin equations. We find that for low temperatures ($T = 30$ K) the oscillations are mostly linear and the frequency density does not differ much from the density of linear modes, as demonstrated in Fig. 2,*b*. However, for higher temperatures ($T = 300$ K) the spectral density acquires specific features associated with the generation of nonlinear modes, as can be seen in Fig. 2,*a* where we observe thermal oscillations with the frequencies inside the linear spectral gaps which can be associated with discrete breathers. Indeed, the larger contribution of these nonlinear modes is for the torsion oscillations of the twisting breathers, which are stable and have the largest frequency spectrum.

We have carried out the similar nonlinear analysis for the nanotubes with the index (m, m) and revealed that in this nanotube can support only one type of breathers, a radial breather with a very narrow frequency spectrum [430.5, 436] cm^{-1} near the upper edge of the frequency

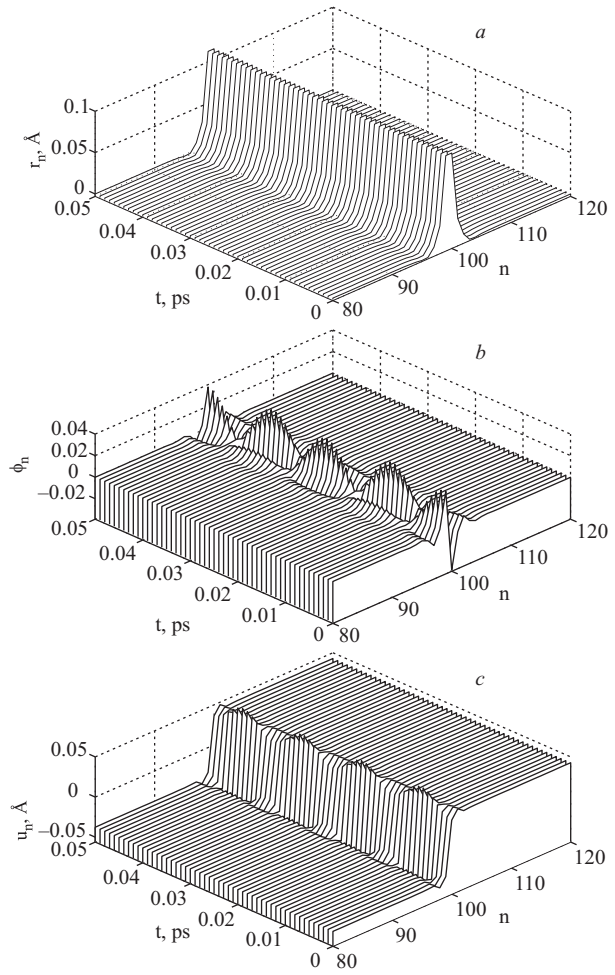

Fig. 4. Dependence of transverse r_n (*a*),) torsion ϕ_n (*b*), and longitudinal u_n (*c*) displacements of the twisting discrete breather (frequency $\omega = 1367$ cm^{-1}, energy $E = 1.6465$ eV, width $L = 1.55$) on the time t.

band of radial phonons. However, this radial breather is not an exact solution of the nonlinear motion equations, and radiation of small-amplitude linear waves leads to a decay of the breather. As a result, the existence of nonlinear localized modes depends crucially on chirality of the carbon nanotube, so that genuine discrete breathers are

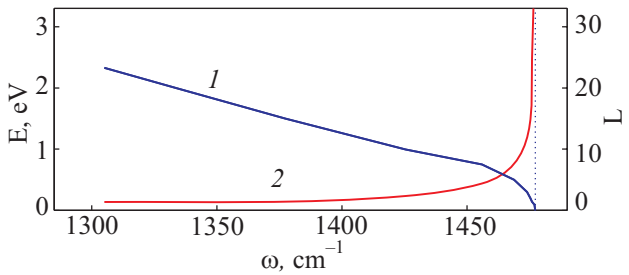

Fig. 5. Dependence of total energy E (curve *1*) and width L (curve *2*) of the twisting discrete breather on the frequency ω Vertical line show the edge of the linear spectrum of optical torsion oscillations in the (10,0) nanotube.

expected to exist in the nanotube with the index (*m*,0). Existence of twisting breathers is due to the anharmonic interaction potential, and the large spectral gap in the frequency spectrum of torsion phonons. However, the radial long-lived nonlinear modes can appear in the nanotubes with any type of chirality.

We have also extended our analysis on the complete three-dimensional model described by not reduced but complete set of equations. This analysis confirmed that the main conclusions of our analysis remain valid, however, the thermalized dynamics of the complete systems demonstrated much richer behavior. Figures 6,*a*–*d* demonstrate several different scenarios of the evolution of the twisting breather. When the coupling to thermostat is absent, ($T = 0$), the twisting breather exists as a stable nonlinear mode even in the complete model (see Fig. 6,*a*). To analyze the interaction of this breather with thermal oscillations, we solve the motion equation with the external random forces and damping (in the form of the Langevin equations for end atoms $1 \le n \le N_0$ and $N - N_0 < n \le N$), and trace the longitudinal distribution of the local temperature

$$T_n = \frac{M}{6mk_B} \sum_{l}^{m} \langle (\dot{\mathbf{x}}_{n,l}; \dot{\mathbf{x}}_{n,l}) \rangle .$$

Figures 6,*b*–*d* show that for $T > 0$ the breather energy slowly distributed along the nanotube, and this defines the lifetime of the excited breather (a few picoseconds, or several hundreds of oscillations).

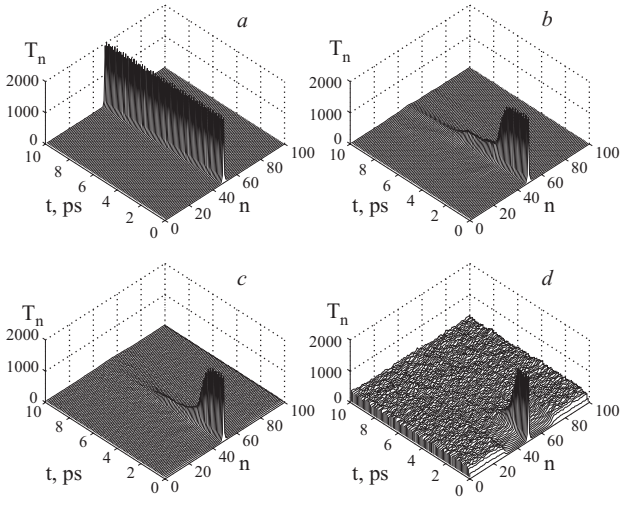

Fig. 6. Thermalized dynamics of the twisting discrete bretaher described by a complete three-dimensional model of the carbon nanotube with the chirality index (*m*,0) (for $m = 10$) ($N = 100, N_0 = 30$) for temperature T, K: 0 (*a*), 3 (*b*), 30 (*c*) and 300 (*d*) (breather frequency $\omega = 1341$ cm^{-1}). Shown is the temporal evolution of the current magnitudes T_n of local temperature (kinetic energy of nanotube segments $(n,l,k)_{l=1,k=0}^{m,1}$).

6. Conclusions

We have studied the nonlinear localized modes in complex atomic structures associated with the geometry of carbon nanotubes. We have revealed that such structures can support spatially localized large-amplitude stable nonlinear modes, and we have analyzed the existence and stability of three types of breathers. A novel type of such highly localized discrete modes — twisting breathers — is associated with the energy self-trapping of torsion oscillations of the carbon nanotubes. We have demonstrated that such type of nonlinear localized modes can be also found in the complete three-dimensional model, beyond the approximation adopted in our analysis. Our numerical results confirm that the curved geometries of carbon nanotubes with the chirality $(m,0)$ supports the existence of strongly localized nonlinear twisting modes with the lifetime of the order of several picoseconds.

This work was supported by the Australian Research Council. Alex Savin thanks the Nonlinear Physics Center of the Australian National University for a warm hospitality during his stay in Canberra.

1. A.M. Kosevich and A.S. Kovalev, *Zh. Eksp. Teor. Fiz*. **67**, 1793 (1974) [*Sov. Phys. JETP* **40**, 891 (1975)].
2. A.J. Sievers and S. Takeno, *Phys. Rev. Lett*. **61**, 970 (1988).
3. S. Flach and C.R. Willis, *Phys. Rep.* **295**, 182 (1998).
4. D.K. Campbell, S. Flach, and Yu.S. Kivshar, *Phys. Today* **57**, 43 (2004).
5. E. Trias, J. Mazo, and T. Orlando, *Phys. Rev. Lett*. **84**, 745 (2000); P. Binder, D. Abraimov, A.V. Ustinov, S. Flach, and Y. Zolotaryuk, *Phys. Rev. Lett*. **84**, 741 (2000).
6. H.S. Eisenberg, Y. Silberberg, R. Morandotti, A.R. Boyd, and J.S. Aitchison, *Phys. Rev. Lett.* **81**, 3383 (1998).
7. M. Sato and A.J. Sievers, *Nature* **432**, 486 (2004).
8. R. Saito, G. Dresselhaus, and M.S. Dresselhaus, *Physical Properties of Carbon Nanotubes*, Imperial College Press, London (1998).
9. S. Iijima, *Nature* (*London*) **354**, 56 (1991).
10. M.M.J. Treacy, T.W. Ebbesen, and J.M. Gibson, *Nature* (*London*) **381**, 678 (1996).
11. S. Berber, Y.K. Kwon, and D. Tomanek, *Phys. Rev. Lett*. **84**, 4613 (2000).
12. A.M. Rao, E. Richter, S. Bandow, B. Chase, P.C. Eklund, G. Dresselhaus, and M.S. Dresselhaus, *Science* **275**, 187 (1997).
13. T. Laarmann, I. Shchatsinin, A. Stalmashonak, M. Boyle, N. Zhavoronkov, J. Handt, R. Schmidt, C.P. Schulz, and I.V. Hertel, *Phys. Rev. Lett*. **98**, 058302 (2007).
14. T.Yu. Astakhova, O.D. Gurin, M. Menon, and G.A. Vinogradov, *Phys. Rev*. **B64**, 035418 (2001).
15. A.V. Savin and O.I. Savina, *Phys. Solid State* **46**, 383 (2004).
16. R.S. MacKay and S. Aubry, *Nonlinearity* **7**, 1623 (1994).
17. R. Al-Jishi and G. Dresselhaus, *Phys. Rev*. **B26**, 4514 (1982).